

# Tree growth declines and mortality were associated with a parasitic plant during warm and dry climatic conditions in a temperate coniferous forest ecosystem

David M. Bell<sup>1</sup>  | Robert J. Pabst<sup>2</sup> | David C. Shaw<sup>3</sup>

<sup>1</sup>Pacific Northwest Research Station, USDA Forest Service, Corvallis, OR, USA

<sup>2</sup>Department of Forest Ecosystems and Society, Oregon State University, Corvallis, OR, USA

<sup>3</sup>Department of Forest Engineering, Resources & Management, Oregon State University, Corvallis, OR, USA

## Correspondence

David M. Bell, USDA Forest Service, Pacific Northwest Research Station, Corvallis, OR, USA.

Email: dmbell@fs.fed.us

## Funding information

Division of Environmental Biology, Grant/Award Number: 1440409; University of Washington; USDA Forest Service

## Abstract

Insects and pathogens are widely recognized as contributing to increased tree vulnerability to the projected future increasing frequency of hot and dry conditions, but the role of parasitic plants is poorly understood even though they are common throughout temperate coniferous forests in the western United States. We investigated the influence of western hemlock dwarf mistletoe (*Arceuthobium tsugense*) on large ( $\geq 45.7$  cm diameter) western hemlock (*Tsuga heterophylla*) growth and mortality in a 500 year old coniferous forest at the Wind River Experimental Forest, Washington State, United States. We used five repeated measurements from a long-term tree record for 1,395 *T. heterophylla* individuals. Data were collected across a time gradient (1991–2014) capturing temperature increases and precipitation decreases. The dwarf mistletoe rating (DMR), a measure of infection intensity, varied among individuals. Our results indicated that warmer and drier conditions amplified dwarf mistletoe effects on *T. heterophylla* tree growth and mortality. We found that heavy infection (i.e., high DMR) resulted in reduced growth during all four measurement intervals, but during warm and dry intervals (a) growth declined across the entire population regardless of DMR level, and (b) both moderate and heavy infections resulted in greater growth declines compared to light infection levels. Mortality rates increased from cooler-wetter to warmer-drier measurement intervals, in part reflecting increasing mortality with decreasing tree growth. Mortality rates were positively related to DMR, but only during the warm and dry measurement intervals. These results imply that parasitic plants like dwarf mistletoe can amplify the impact of climatic stressors of trees, contributing to the vulnerability of forest landscapes to climate-induced productivity losses and mortality events.

## KEYWORDS

*Arceuthobium tsugense*, climate, dwarf mistletoe, growth, mortality, Pacific Northwest United States, tree, *Tsuga heterophylla*, western hemlock

## 1 | INTRODUCTION

Increasing stress under hot and dry conditions is, among other things, likely to reduce tree growth and increase tree mortality rates in the western United States (Allen, Breshears, & McDowell, 2015),

but the consequences of drought on stands, landscapes, and regions depend on tree-level interactions between stress agents such as climate and natural enemies (Agne et al., 2018; Clark et al., 2016; Kolb et al., 2016). Regional assessments of disturbance rates have indicated an increase in the prevalence of slow and subtle changes

in forest canopies in the western United States associated with drought (Cohen et al., 2016). However stand-level variation in the sensitivity of forests to drought implies that local biotic factors likely play a strong role in amplifying or dampening vulnerability (Bell, Cohen, Reilly, & Yang, 2018). For example, defoliator or bark beetle attacks may alter the impact of drought on tree mortality (Birch et al., 2019; Hogg, Brandt, & Michaelian, 2008), possibly related to long-term changes in physiological response to drought (Hillabrand et al., 2019). In contrast, some pathogens may be facilitated by wet and warm conditions, as indicated by the relationship between satellite-based forest stress measurements and the distribution and expansion of Swiss needle cast (*Phaeocryptopus gaeumannii*), a common leaf pathogen for young Douglas-fir trees (*Pseudotsuga menziesii*; Mildrexler, Shaw, & Cohen, 2019). Similarly, parasitic plants, such as dwarf mistletoe (*Arceuthobium* species), likely increase the sensitivity of coniferous tree species to drought (Dobbertin & Rigling, 2006; Stanton, 2007). In contrast to insects and fungal pathogens, the role of parasitic plants in mediating tree responses to drought at the ecosystem level is still poorly understood (Way, 2011).

While drought may not impact parasitic plants in the same manner as host plants, trees that are infected may be predisposed to drought-related reductions in vigor, resulting in branch death, top dieback, and even whole-tree mortality (Kliejunas, 2009; Kolb et al., 2016). Dwarf mistletoe infection level is typically determined on a six-class dwarf mistletoe rating (DMR) system, with 0 meaning no infection and 6 meaning the tree is heavily infected throughout the crown (Hawsworth, 1977; Hawsworth & Wiens, 1996). The relative reduction in radial growth of infected trees compared to uninfected trees ranged from 5% to 20% for DMR class 4 up to 41%–66% for DMR class 6 (Hawsworth & Wiens, 1996). The same authors found a commensurate increase in tree mortality rates with increased mistletoe infection. Thus, DMR provides useful information regarding the impacts of dwarf mistletoe infection on tree growth and mortality processes, such that heavy infections in conifers have the greatest impact (Hawsworth & Wiens, 1996; Mathiasen, Nickrent, Shaw, & Watson, 2008). Drought can exacerbate the effects of dwarf mistletoe infections, as well as predispose infected conifers to impacts by other mortality agents such as bark beetles (Hawsworth & Wiens, 1996; Kolb et al., 2016).

Forests across much of the northwestern United States can be highly productive (Gray & Whittier, 2014) due in part to a generally wet and mild climate (Waring & Franklin, 1979), leading some to speculate that forest vulnerability to drought is most likely in drier regions as opposed to these wet forests (e.g., Chmura et al., 2011). However, drought-induced forest declines have been observed in all forest biomes, leading others to argue that forest ecologists may be underestimating the degree to which drought-induced forest change might occur under future climate change, especially in wet forest ecosystems (Allen et al., 2015). Given that many tree species already operate within relatively narrow hydraulic safety margins, reductions in productivity and survival associated with drought may become common under climate change in wet forests not normally

considered at risk from drought (Choat et al., 2012). Interactions between trees and their natural enemies, such as parasitic plants, could amplify drought-induced reductions in productivity and survival.

*Arceuthobium tsugense* (western hemlock dwarf mistletoe) is a native parasitic plant infecting western hemlock (*Tsuga heterophylla*; Muir & Hennon, 2007) potentially capable of amplifying the effects of drought on forest ecosystems. Projectile seed from aerial shoots of *A. tsugense* generally land on and infect 5 year or younger branches by penetrating the cambium, eventually inducing branch swelling, branch deformation, and new aerial shoot development from which further infection can progress (Hawsworth & Wiens, 1996). *Arceuthobium tsugense* occurs in distinct infection centers associated with stand age and disturbance history, often being abundant in the oldest forests (Shaw, Chen, Freeman, & Braun, 2005; Swanson, Shaw, & Marosi, 2006). Infection can have substantial impacts on tree physiology, and thus productivity and survival. Infected *T. heterophylla* exhibited maximum whole-tree water use of about 55 kg/day in heavily infested (DMR 6) trees versus 90 kg/day for uninfected trees; this difference was likely due to reductions in the number of live branches for infected trees (Meinzer, Woodruff, & Shaw, 2004). Mesophyll conductance in infected compared to uninfected trees was lower and path length for water movement was higher in needles (Marias et al., 2014), highlighting physiological changes due to pathogen infection. Long-term (1886–2010) diameter growth comparisons indicated that initially, infected trees grew faster, but as the infection intensified the tree growth and leaf-level photosynthetic capacity declined compared with uninfected trees (Marias et al., 2014). Furthermore, heavily infected *T. heterophylla* trees (DMR 5–6) showed significant departures from DMR 0, with growth reduction averaging 36% (16%–46%; Shaw, Huso, & Bruner, 2008). These results imply that *A. tsugense* may alter *T. heterophylla* sensitivity to other stressors, such as heat or moisture stress.

In this research, we asked the following question: How do *A. tsugense* and shifting climate interact to alter growth and mortality patterns in *T. heterophylla* trees distributed across a coniferous forest landscape in western Washington, United States? At Wind River Experimental Forest (WREF), we used long-term tree measurements (1991–2014) to (a) quantify effects of *A. tsugense* on individual tree growth and mortality and (b) explore the potential contribution of hot and/or dry conditions to observed patterns. We hypothesized that growth reductions and mortality would increase as *A. tsugense* infection severity increased and that the magnitude of those changes would be greatest during measurement intervals characterized by greater temperatures and/or lesser precipitation.

## 2 | MATERIALS AND METHODS

### 2.1 | Study site

The study site is located at the T. T. Munger Research Natural Area (MuRNA; established 1934), a 478 ha old-growth Douglas-fir (*Pseudotsuga menziesii*) and western hemlock forest (Figure 1) with

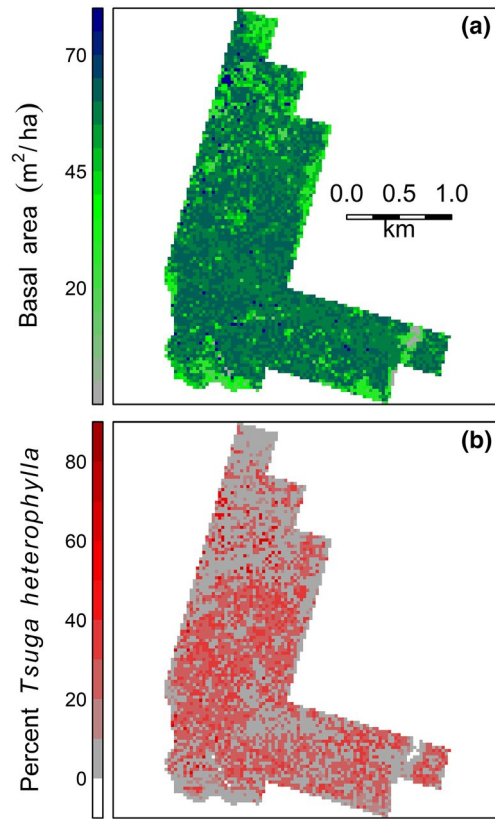


**FIGURE 1** Map of forest conditions for the study area. We present (a) tree basal area and (b) percentage of basal area attributed to western hemlock (*Tsuga heterophylla*) for the T. T. Munger Research Natural Area within the Trout Creek Division of the Wind River Experimental Forest, Washington, United States. Basal area data were extracted from the 2012 gradient nearest neighbor vegetation mapping product (Davis et al., 2015; Kennedy et al., 2018)

the oldest trees estimated to be about 500 years of age (Shaw et al., 2004; Swanson et al., 2006) and the oldest *T. heterophylla* estimated to be 300 years of age (North et al., 2004). The MuRNA is located within the WREF (Shaw & Greene, 2003), part of the Gifford Pinchot National Forest in southwestern Washington state, United States. Other tree species present include western redcedar (*Thuja plicata*), grand fir (*Abies grandis*), Pacific silver fir (*A. amabilis*), noble fir (*A. procera*), and Pacific yew (*Taxus brevifolia*). Understory vegetation varies across the study area, but is generally dominated by vine maple (*Acer circinatum*), salal (*Gaultheria shallon*), Oregon grape (*Mahonia nervosa*), with foamflower (*Tiarella trifoliata*) and lady fern (*Athyrium filix-femina*) on moister sites. Elevation ranges from 335 to 610 m with gently sloping topography that is not deeply incised. The MuRNA is on the east and south sides of Trout Creek Hill, a ~340,000 year-old basaltic shield volcano. Soils are deep, well-drained, and generally stone free, having a tephra parent material (Shaw et al., 2004).

## 2.2 | Field observations

Within the MuRNA, we leveraged data from ninety-four 0.4 ha forest inventory plots distributed across the study site along nine

transects spaced 401 m apart (Shaw et al., 2005; Shaw & Franklin, 2019; Swanson et al., 2006). In 1991, all trees  $\geq 45.7$  cm diameter at breast height were tagged to aid in repeated measurements of individuals. Within each plot, tagged trees were surveyed for tree species, diameter, and survival status in 1991, 1998, 2004, 2009, and 2014. Note that negative diameter changes observed for some trees during some measurement intervals (3% of all remeasurements) can likely be attributed to the methodological factors (e.g., measurement uncertainties for large diameter trees) and biological factors (e.g., bark sloughing).

In 1997, 1,395 western hemlock trees were rated for dwarf mistletoe infection using the six-class DMR system (Hawksworth & Wiens, 1996). Tree crown was divided into thirds and each third was assigned a rating: 0 (no branches infected), 1 (<50% of branches with an infection), or 2 (>50% of the branches with an infection). The numbers assigned to each third were summed to produce a DMR rating for each individual tree. Because DMR was surveyed only once, we assumed that the 1997 measurement is representative of the infection conditions through time. Spread and intensification of dwarf mistletoe are controlled by stand composition, density, and structure (e.g., light environment for growth and distance between trees and limbs for spread; Robinson & Geils, 2006). Spread and intensification are thought to occur relatively slowly (Muir & Hennon, 2007). For example, it may take 3–5 years from seed infection of a twig to the emergence of aerial shoots and flowering, while explosive discharge of seed from the fruit limits the distance of vertical and horizontal spread (Hawksworth & Wiens, 1996; Muir & Hennon, 2007). Dwarf mistletoe intensification rates for *P. menzeisii* in New Mexico were observed for increases in 0.5 DMR per decade for large canopy trees (Geils & Mathiasen, 1990). Simulation modeling of *A. tsugense* dynamics at our study site indicated that while the number of infected trees may have increased from 25% to 40%, the average DMR rating likely did not increase during 1995–2015 (Robinson & Geils, 2006). Therefore, the DMR ratings recorded in 1997 probably underestimate DMR in 2014, but the large size of study trees ( $\geq 45$  cm diameter) may minimize DMR changes during the study period.

## 2.3 | Climate data

To characterize patterns of climatic conditions during the study period (1991–2014), we extracted mean annual temperature (MAT; °C) and mean annual precipitation (MAP; mm) from the 30 arc sec (approximately 800 m) resolution data from the Parameter-elevation Regressions on Independent Slopes Model (PRISM; Daly et al., 2008; PRISM Climate Group, 2018). We extracted annual data for all pixels that overlapped MuRNA and calculated MAT and MAP for each of the four tree measurement intervals: 1991–1997, 1998–2003, 2004–2008, and 2009–2013, using the means across pixels and years. We also extracted data for 1970–1990 as a measure of historical conditions prior to tree measurements. Finally, we calculated means and 95% confidence intervals for 1970–1990 and each measurement interval to assess changes in MAT and MAP through time. Note that for the purposes of summarizing nonoverlapping climate

data, we defined a measurement interval as beginning with a tree measurement year and ending the year before the subsequent tree measurement year (e.g., tree measurement interval of 1991–1998 has a climate measurement interval of 1991–1997). All manipulations of raster data, including the preparation of climate data used the raster package version 2.6-7 (Hijmans & van Etten, 2011) in the R statistical programming environment version 3.5.1 (R Development Core Team, 2016).

## 2.4 | Tree growth and mortality analyses

For this study, we examined how dwarf mistletoe infection, as indicated by DMR, was related to individual *T. heterophylla* growth and mortality rates through time. We assumed that DMR had a direct impact on tree growth (Shaw et al., 2008). Additionally, we characterized the relationship between tree growth and mortality (i.e., vigorously growing trees often have lower risk of mortality; Das & Stephenson, 2015; Das, Stephenson, & Davis, 2016; Kobe, 1996) and explored mistletoe's effects on mortality as mediated through its effects on growth (i.e., indirect DMR effect on mortality). We then examined how the relationship of DMR to growth and mortality varied between different measurement intervals: 1991–1998, 1998–2004, 2004–2009, and 2009–2014. Note that these intervals differ slightly from those of climate data because climate data were aggregated by calendar years (i.e., nonoverlapping), whereas growth and mortality represent all changes occurring between one tree measurement and the next.

To quantify the DMR effect on *T. heterophylla* growth, we developed a hierarchical Bayesian mixed-effects regression model to account for the effect of dwarf mistletoe infection (DMR) and plot-level factors (e.g., soils, topography, etc.) on individual tree growth patterns for each measurement interval. We considered three different metrics of growth (annualized diameter increment (cm/year), annualized basal area increment (m<sup>2</sup>/year), and annualized relative basal area increment (%/year)) and determined the most appropriate for further analysis based on a model selection procedure described below. To account for variation in growth between plots driven by abiotic (e.g., soils, topography) and biotic (e.g., stand density) factors other than DMR, we incorporated a plot-level random effect in the growth process. Thus, for each individual *i* on plot *j* during the interval ending in year *t*,  $y_{ij,t}$  was tree growth and was modeled as a normally distributed random variable, such that:

$$y_{ij,t} \sim N\left(\beta + \sum_{k=1}^6 \alpha_k I(\text{DMR}_{ij} = k) + \gamma_j, \sigma^2\right), \quad (1)$$

where  $\beta$  is the mean growth rate for an uninfected tree,  $\alpha_k$  is the growth effect for trees with DMR equal to *k* (i.e., the difference between mean growth for an uninfected tree and a tree with  $\text{DMR}_{ij} = k$ ),  $I(\text{DMR}_{ij} = k)$  is an indicator equal to one when the DMR for tree *ij* equals *k* and zero otherwise,  $\gamma_j$  is the plot-level random effect for plot *j*, and  $\sigma^2$  is the variance. The random effects were

modeled as  $\gamma_j \sim N(0, \tau^2)$ . For the regression parameters  $\beta$  and  $\alpha_k$ , we assumed weak prior distributions of  $N(0, 10,000)$ . For  $\sigma^2$  and  $\tau^2$ , the process and random effect errors, respectively, we assumed weak prior distributions of  $\text{Gamma}^{-1}(0.01, 0.01)$ .

To examine temporal trends in *T. heterophylla* mortality, we developed a hierarchical Bayesian logistic regression model for mortality as a function of previous growth rates for 1998–2004, 2004–2009, and 2009–2014. Mortality for 1991–1998 was not modeled as we had no prior growth data (pre-1991) upon which to base the analysis. In this case, we modeled observations of mortality ( $z_i = 1$ ) and survival ( $z_i = 0$ ) as:

$$z_i \sim \text{Bernoulli}\left(1 - (1 - \theta_i)^{\text{dt}}\right), \quad (2)$$

$$\text{logit}(\theta_i) = \delta_0 + \delta_1 y_i, \quad (3)$$

where  $\text{logit}(p) = \log(p/(1 - p))$ ,  $\delta_0$  is an intercept parameter,  $\delta_1$  is a growth effect parameter,  $\text{dt}$  is the length of the measurement interval in years, and  $y_i$  is the growth during the previous time interval (e.g., mortality during 1998–2004 affected by growth for 1991–1998). Again, we standardized for the length of measurement intervals to calculate annual rates, mortality in this case. Note that we exclude subscripts for plot (*j*) for simplicity as plot-level random effects were not included. For the regression parameters  $\delta_0$  and  $\delta_1$ , we assumed weak prior distributions of  $N(0, 10,000)$ . Plot-level random effects and fixed effects for DMR were not included because some combinations of plot or DMR with year yielded zero observed tree deaths, making parameter estimation difficult. This was likely due to the fact that only 128 tree deaths were observed during the entire study period (Table S1). Instead, plot-level and DMR effects were assumed to be incorporated in the effect of tree growth. Because of the apparent effects of DMR infection on growth, including DMR in the model of mortality could cause issues with multicollinearity because DMR and growth represent similar information. We assumed that growth was a measure of tree vigor (Das et al., 2016; Kobe, 1996), with *A. tsugense* negatively impacting growth (as indicated by the tree growth modeling). In our modeling framework, for *A. tsugense* infections to impact mortality, (a) DMR must reduce growth rates and (b) growth must be negatively related to the probability of mortality. Note that all dead trees were used for modeling, regardless of the recorded cause of death (Table S1).

Previous studies have indicated that the selection of growth metric contributes to mortality model performance (Das & Stephenson, 2015), so we examined three metrics of tree growth: annualized tree diameter increment (cm/year), annualized tree basal area increment (m<sup>2</sup>/year), and percentage annualized tree basal area increment (%/year). We fit mortality models using each of these growth metrics in the logit function (Equation 3) as well as tree diameter as a measure of size effects. We assessed performance based on minimizing the deviance information criteria, an information theoretic approach for complex, hierarchical models (Spiegelhalter, Best, Carlin, & Van Der Linde, 2002). Mortality models with diameter increment only performed best (minimum deviance information criteria) for two

measurement intervals (2004–2009, 2009–2014) or were equivalent (deviance information criteria 0.1 greater than minimum) to the best performing model (1998–2004; Table S2). In favor of parsimony and a consistent model structure for all measurement intervals, we report results associated with models incorporating diameter increment, either as a response variable for the growth modeling (i.e.,  $y_{i,j}$  = diameter increment [cm]; Equation 1) or as the sole predictor variable for the mortality modeling (i.e.,  $y_i$  = previous diameter increment [cm]; Equations 2 and 3).

In this work, we did not explicitly account for specific mortality agents. Several factors may predispose individual trees to elevated mortality risk and can be difficult to separate. Therefore, we used the relationship between tree mortality and growth as our primary method of determining the potential effects of DMR on the mortality process. To assess the relative contributions of changes in growth (which may be related to DMR) on the predicted mortality rates (i.e., what percentage of increased mortality is due to decreased growth during stressful measurement intervals), we calculated mean predicted mortality rates for each individual tree based on the mortality model (Equations 2 and 3) from a high mortality period (2009–2014) and individual observed diameter increments during low mortality (1998–2004) and high mortality (2009–2014) periods. The relative contribution of tree growth reductions to elevated mortality ( $R$ ) was then calculated as the percent difference between (a) the mean predicted mortality across all live trees in 2009–2014 conditioned on the previous period's observed growth (2004–2009;  $M_1$ ) and (b) the mean predicted mortality across all live trees in 2009–2014 conditioned on observed growth from earlier measurement intervals during which low mortality was observed (1998–2004;  $M_2$ ;  $R = [M_1 - M_2]/M_1$ ). Thus,  $M_1$  represents the predicted mortality rates and  $M_2$  represents the predicted mortality rates independent of the observed growth reductions.

Both growth and mortality models were fit to the data using a Gibbs sampler within JAGS version 4.2.0 (Plummer, 2016) within the R statistical programming environment version 3.5.1 (R Development Core Team, 2016) using rjags version 4-6 (Plummer, 2014). Models were independently fit for each measurement interval. Convergence was determined visually for four independent model runs. For the growth model, the Gibbs sampler was run for 170,000 iterations, discarding the first 120,000 iterations for parameter estimation. For the mortality models, the Gibbs samplers were run for 40,000 iterations, discarding the first 20,000 iterations for parameter estimation.

### 3 | RESULTS

During the last several decades, the climate at our study area has grown warmer and drier (Figure 2). Compared to the 1970–1990 climate, MAT was greater during all four measurement intervals, with the greatest differences observed for 2004–2008, followed by 2009–2013. Confidence intervals for MAT for measurement intervals after 2004 did not overlap with MAT for 1970–1990. MAP was less than 1970–1990 during three measurement intervals

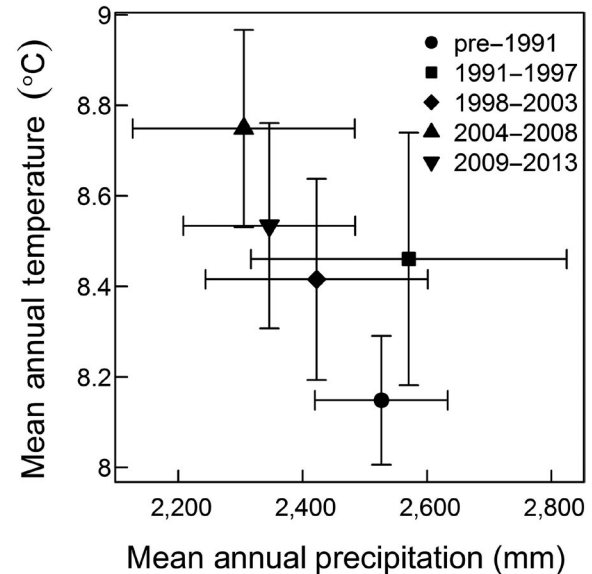


**FIGURE 2** Mean annual precipitation (mm) and temperature (°C) with 95% confidence intervals for the T. T. Munger Research Natural Area within the Trout Creek Division of the Wind River Experimental Forest. Each interval is based on nonoverlapping, consecutive years associated with the 20 year preceding study establishment (1970–1990), and each tree measurement interval (e.g., first measurement year 1991 to the year before the second measurement year 1998)

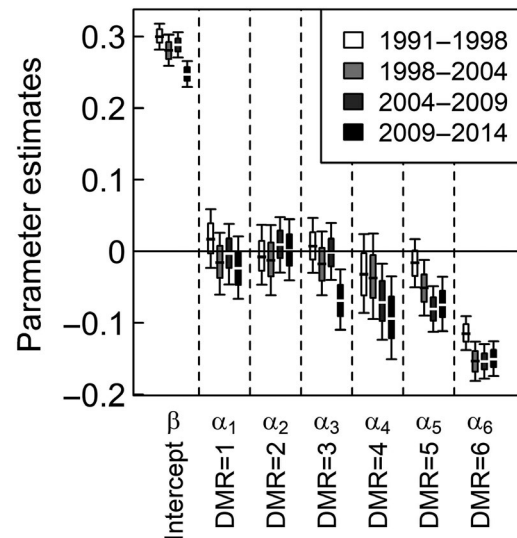


**FIGURE 3** Regression parameter estimates from the growth modeling (Equation 1) indicated decreasing growth across measurement intervals ( $\beta$ ; intercept) as well as increasingly negative effects of dwarf mistletoe infestations ( $\alpha_k$ ; effect of dwarf mistletoe rating =  $k$ ) during the study period. We present mean (horizontal bar), 68% credible intervals (box), and 95% credible intervals (whiskers) for the parameter estimates (see Table S3)

(1998–2003, 2004–2008, and 2009–2013). However, these differences were not statistically strong, with 95% confidence intervals overlapping 1970–1990 conditions. The 2004–2008 measurement interval exhibited the greatest changes compared to the 1970–1990



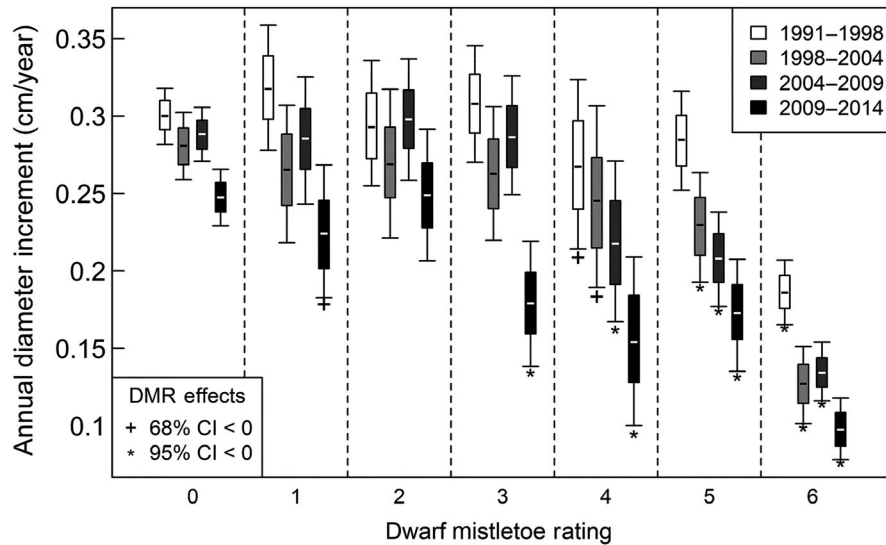


**FIGURE 4** Mean annual growth for *Tsuga heterophylla* decreased with dwarf mistletoe rate and measurement interval. We present mean (horizontal bar), 68% credible intervals (box), and 95% credible intervals (whiskers) for annual diameter increment for each dwarf mistletoe rating (0 = uninfected, 6 = heavily infected) and measurement. Growth reductions associated with a given dwarf mistletoe rating level (68% and 95% credible intervals less than zero for the growth modeling parameter estimates in Figure 3) are indicated by '+' and '\*', respectively

averages, with an increase in MAT of 0.6°C and a decrease in MAP of 220 mm.

Regression parameters for the growth modeling indicated that growth declined throughout the study period ( $\beta$ ; intercept) and that the effect of DMR on growth ( $\alpha_k$ ; effect of DMR =  $k$ ) tended to become more negative later in the study period (Figure 3). The presence of differences in model parameter estimates between measurement intervals for both the intercept and the DMR effects indicate an interactive relationship of measurement interval and DMR on growth. The differences in DMR effect across measurement intervals appear most obvious for intermediate to heavy infections (DMR 3–5), whereas low infections (DMR 1–2) and the heaviest infections (DMR 6) do not appear to show a difference in parameter estimates across measurement intervals.

Mean annual diameter increment for *Tsuga heterophylla* decreased with DMR and measurement interval (Figure 4). Heavily infected trees exhibited less growth compared to uninfected trees during all measurement intervals, as indicated by growth effects for DMR = 6 that were less than zero during all measurement intervals ( $\alpha_6 < 0$ ; Figure 3 and Table S3). Moderately to heavily infected trees (DMR 3–5) exhibited less growth compared to uninfected (DMR 0) and lightly infected (DMR 1–2) trees only during later measurement intervals, especially 2009–2014. Even some growth effect in lightly infected trees (DMR = 1) was observed during 2009–2014. Regardless of DMR, *T. heterophylla* growth tended to decrease during successive measurement periods by 20%–50%, depending on the DMR rating.

Examination of observed annual mortality rates indicated that the greatest mortality rates were associated with heavily infected trees during later measurement intervals (Figure 5). During most measurement intervals, tree mortality was greatest in heavily infected trees

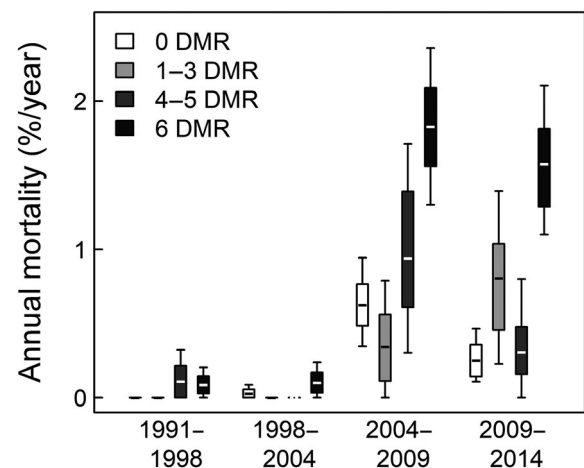


**FIGURE 5** Observed mean annual mortality rates for each measurement interval grouped by dwarf mistletoe rating (DMR) classes: uninfected (DMR = 0), light to moderate infection ( $1 \leq \text{DMR} \leq 3$ ), moderate to heavy infection ( $4 \leq \text{DMR} \leq 5$ ), and heavy infection (DMR = 6). We present mean (horizontal bar), 68% credible intervals (box), and 95% confidence intervals (whiskers) based on nonparametric bootstrapping

(DMR = 6), with mortality rates associated with moderate infection similar to or greater than rates for uninfected trees. Mean annual mortality rates across all DMR levels were near zero ( $\leq 0.1\%$ ) for the first two measurement intervals (1991–2004) and ranged from 0.2% to 1.8% during the final two measurement intervals (2004–2014).

Within a measurement interval, tree mortality rates decreased as growth rates during the previous measurement interval increased, but mortality rates were greatest after 2004 compared to the 1998–2004 interval (Figure 6). For low to moderate annual

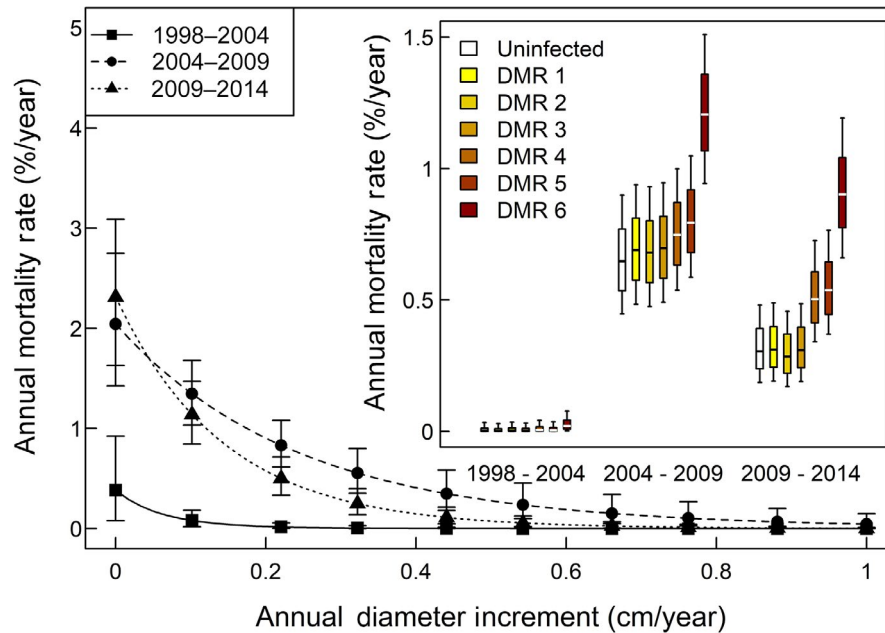


**FIGURE 6** Mortality rates were greatest when diameter increment was low (i.e., slow growth) and during later measurement intervals. Mean and 95% credible intervals for the predicted probability of *Tsuga heterophylla* annual mortality as a function of diameter increment during the previous measurement interval for 1998–2014. Inset: for three measurement intervals, we present the mean (horizontal line), 68% credible interval (box), and 95% credible interval (whiskers) for the predicted annual mortality rates for uninfected and dwarf mistletoe rating 1–6 trees based on their mean predicted growth rates for the previous interval

diameter increment (i.e., <0.3 cm/year, representing 70% of the observations), mortality rates were consistently greater in 2004–2008 and 2009–2014 compared to 1998–2004, reflecting the near complete lack of mortality prior to 2004. Based on the mean growth rate for each DMR class, we found that the heaviest *A. tsugense* infections (DMR = 6) were associated with increased mortality rates in 2004–2009 and 2009–2014, while moderate to heavy infections (DMR 4–5) were associated with increased mortality rates for the period 2009–2014 (Figure 6, inset). Comparing the last hot and dry period (2009–2014) to the cooler wetter period (1998–2004), mortality increases for greater DMR ratings were as much as double to that of uninfected or lightly infected trees. The relative contribution of declining growth to the changes in mortality between the low and high mortality periods was  $R = 23\%$  ( $M_1 = 0.79\%$  and  $M_2 = 0.61\%$ ).

## 4 | DISCUSSION

### 4.1 | Changing effect of dwarf mistletoe on tree growth and mortality

This study implies that *A. tsugense* may become an increasingly important contributor to tree growth losses and mortality of *T. heterophylla* at the T. T. Munger Research Natural Area in southern Washington, and perhaps in the Pacific Northwest United States more broadly, under increasingly warm and dry climatic conditions. Changes observed in the role of *A. tsugense* on *T. heterophylla* growth from 1991 to 2014 indicated both declining tree growth for all trees

(i.e., decreasing intercepts in the growth model) and increasing growth sensitivity of individual trees to *A. tsugense* infection (i.e., increasing magnitude of DMR effects on growth; Figures 3 and 4) coincident with elevated temperature and reduced precipitation. During our study period, the hottest and driest conditions (2004–2014; Figure 2) were associated with reduced growth for *T. heterophylla*, most notably for those trees with moderate to heavy *A. tsugense* infections (Figure 4). The increasing magnitude of growth reductions associated with dwarf mistletoe are consistent with tree-ring analysis of *Pinus ponderosa* growth indicating that *Arceuthobium* sp. infection increased radial growth sensitivity to climatic variation (Stanton, 2007). Given that the cooler and wetter portions of our study period exhibited reduced growth only for the most heavily infected individuals (DMR 6; Shaw et al., 2008), our results imply both a general reduction in tree vigor and an increasing effect of *A. tsugense* infection as temperature increases and precipitation decreases.

The increasing effects of *A. tsugense* infection on tree mortality during hotter and drier measurement intervals indicated that *A. tsugense* may play an important role as a predisposing factor for climate-induced mortality (Kliejunas, 2009). During hot and dry conditions, mortality rates increased for all hemlock trees regardless of the growth rate (Figures 5 and 6). Predicted mortality rates based on the joint effects of dwarf mistletoe on growth and growth on mortality (Figure 6, inset) were consistent with observed increases in mortality rates for trees infected by dwarf mistletoe (Figure 5). Interestingly, while predicted mortality for moderate to heavy infection levels (DMR 4–5) was only elevated during the final measurement interval (2009–2014), observed mortality for this group was

elevated during the previous period (2004–2009). The 2004–2009 measurement interval exhibited the greatest increases in temperature and decreases in precipitation (Figure 2), potentially indicating greater climatic stress during the penultimate measurement interval. These results imply that *A. tsugense* impacts on mortality may be associated with both long-term declines in vigor and short-term increases in susceptibility. It is important to note that other mortality agents were at work in these stands. For example, a large percentage of the mortality observed was attributed to wind (40% of dead trees; Table S1), though multiple agents likely contributed to tree decline and death. Finer temporal resolution in tree growth data, such as tree ring measurements, could provide an improved capacity to separate short- and long-term dynamics in tree responses to dwarf mistletoe (sensu; Stanton, 2007). Such information would be necessary to disentangle the impacts of chronic stress driven by long-term shifts in climatic normals versus acute stress from short-term events, such as heat waves, droughts, or windstorms.

It is estimated that about 10% of the western hemlock trees in Oregon and Washington are infected with *A. tsugense*, and about 5% have a DMR  $\geq 3$  (Muir & Hennon, 2007). We observed amplification of growth declines and mortality responses to both heavy (DMR 5–6) and moderate (DMR 3–4) *A. tsugense* infection (Figures 3–6) during warmer and drier measurement intervals (2004–2014; Figure 2). During the latter two measurement intervals, mortality rates were well in excess of previously reported rates for this forest (0.59%) for the period 1947–1983 (Franklin & DeBell, 1988). Thus, it appears that in our study landscape, the amplification of tree-level growth declines and mortality associated with moderate to heavy dwarf mistletoe infection coincided with hotter and drier climatic conditions (2004–2014). Furthermore, changes in mortality associated with measurement intervals, and perhaps climate, were as large as or larger than changes associated with DMR infection status. These results are consistent with the idea that trees operate within narrow physiological safety margins (Choat et al., 2012), and that warmer and drier climatic conditions emerging over relatively short time scales are likely to push trees beyond key physiological thresholds and alter forest landscape function (Allen et al., 2015).

*Arceuthobium tsugense* is known to cause host tree growth reductions, branch deformation, branch death, partial crown death (top kill), and mortality (Muir & Hennon, 2007). The impacts on an individual tree intensify as the abundance of *A. tsugense* plant infections accumulate in the crown, though the impacts on growth may take decades to emerge after infection becomes more severe (Marias et al., 2014). Furthermore, parasitic plant infection can dampen other factors that ameliorate drought impacts, such as the combined effects of drought and mistletoe reversing CO<sub>2</sub>-induced increases in water use efficiency in Scots pine (*Pinus sylvestris*; Sangüesa-Barreda, Linares, & Julio Camarero, 2013). Other biotic agents in other forest ecosystems have been implicated, along with co-occurring heat waves and/or drought, as contributing factors for major mortality events, such as bark beetle (*Ips confusus*) attacking pinyon pine (*Pinus edulis*) in the Southwest United States (Allen et al., 2010; Lloret & Kitzberger,

2018), and some mortality events only emerge several decades after the biotic agent has passed (Haavik, Billings, Guldin, & Stephen, 2015). In western Canada mixed aspen forests, drought had a stronger influence on tree growth declines than insect attack, though warm spring conditions may trigger insect outbreaks, further exacerbating growth declines and tree death (Chen et al., 2018). Events like these often far exceed the observed increases in mortality described in this study. However, relatively small changes in mortality, when observed over long periods of time characterized by chronic stress, compound over time and drive substantial changes in forest structure, composition, and function.

Other studies show linkages between dwarf mistletoe and tree growth or mortality, some of which also explore how infection may make trees more vulnerable to environmental stress, such as drought (Griebel, Watson, & Pendall, 2017; Kolb et al., 2016). For example, Sangüesa-Barreda, Linares, and Camarero (2012) demonstrated that basal area increment of *Pinus sylvestris* trees severely infested with *Viscum album* (Viscaceae) diverged from moderately or uninfested trees under drought effect, and they concluded that the sensitivity of trees to drought stress was increased by mistletoe infection. Fontúrbel, Lara, Lobos, and Little (2018) have shown that mistletoe plant (*Tristerix corymbosus*; Loranthaceae) mortality increased from 12% to 23% during a major drought in Chile, with similar results observed for other parasitic plants (Reid & Lange, 1988; Spurrier & Smith, 2007). However, we are unaware of any other direct examination of growth and mortality responses to dwarf mistletoe and climate utilizing repeated measurements of the same trees over the course of decades, which can elucidate the long-term consequences of infection on tree populations. The interactive effects of climatic stress and biotic agents are not well understood, contributing to a major disconnect between our understanding of individual-level tree responses to, for example, drought, and the behavior of forest stands or landscapes (Clark et al., 2016).

## 4.2 | Landscape implications of biotic agent attack

Given that insect and disease prevalence can be high—for example, *A. tsugense* infects 10% of *T. heterophylla* in western Oregon, United States (Muir & Hennon, 2007)—the amplification of drought effects on forests by biotic agents could be widespread. Reassessing assumptions regarding the geographic distribution of forest vulnerability to drought indicate that the current consensus—that is, forest vulnerability to drought declines from dry to wet climates—may underestimate the potential for elevated tree mortality and forest die-off during unusually warm and dry climatic conditions (Allen et al., 2015). While this study was restricted to the WREF and did not examine geographic variation in vulnerability, it did highlight the potential for multidecade trends in temperature and precipitation to interact with local biotic agents to reduce tree growth and increase tree mortality in wet forest ecosystems. For example, laminated root rot, as well as other root rot fungi, can cause a speedy or slow decline of the tree, and may persist on roots of live trees



for decades depending on tree age (Hansen, Lewis, & Chastagner, 2018). It is generally hypothesized that trees with existing root rot infections would be less able to tolerate drought stress, and that heat and drought would disproportionately impact trees with existing root rot. Additionally, other natural enemies might focus attacks on trees infected by pathogens during nonoutbreak conditions, as seen with *Dendroctonus pseudotsugae* (Douglas-fir beetle; *Coleoptera: Curculionidae*) attack on Douglas-fir infected with laminated root rot (Agne et al., 2018). These coinfection patterns indicate that the trees may lack the ability to repel attack presumably due to compromised function. Therefore, chronic insect and disease attack present in the current forest ecosystems may be a contributor to future forest vulnerability to growth reductions and mortality.

Because we were examining a single landscape, we cannot rule out the potential role of some unknown process or stressor contributing to the recent changes in DMR impacts on growth and mortality. Furthermore, we did not have access to long-term data for small to moderate size trees (<45 cm diameter), which may experience (a) greater infection rates and (b) greater competition for light and soil water (Robinson & Geils, 2006). Therefore, additional research is needed to assess whether interactions between multiple biotic agents and drought emerge in forests across broader gradients of temperature and moisture conditions and whether such responses depend on tree size class distributions.

### 4.3 | Confounding factors

Potential climatic and dwarf mistletoe effects on tree growth and mortality reported in this study may be confounded with several factors, including the intensification of *A. tsugense* infections over time, tree aging during the study period, or the prevalence of other mortality agents unrelated or weakly related to dwarf mistletoe infection. However, it seems unlikely that infection intensification or tree aging explain our results completely. Previous work implies that DMR may have changed little over two decades (Geils & Mathiasen, 1990; Robinson & Geils, 2006) and while increases of 1.0 DMR were likely at our study site, it is unlikely that, for example, transitions from DMR 3 to DMR 6 would be common from 1997 to 2014. For 300 year old *T. heterophylla* at our study site (North et al., 2004), the 23 year study period is short compared to the ages of the trees, likely limiting changes in tree demography as a function of age alone.

In contrast, the observed mortality patterns (Figure 5) indicate that the contribution of differing agents may play an important role in the interpretation of our results. Most notably, wind-related tree mortality can be substantial in old-growth forests of the Pacific Northwest United States (Franklin, Shugart, & Harmon, 1987). In our study, 43% of the dead western hemlock was associated with some form of mechanical mortality (i.e., wind, crushing, or stem breakage, Table S1) and 89% of that mechanical mortality occurred between the 2004 and 2009 measurements. This coincides with a December 2006 'Hanukkah Eve' storm that generated high winds

along the Columbia River Gorge near our study site. However, no wind mortality was observed from 2009 to 2014, which exhibited similar mortality rates as 2004–2009. Thus, wind might explain the minor differences in predicted mortality rates between the final two measurement intervals (2004–2009 > 2009–2014; Figure 6), but perhaps not majority of the elevated mortality in these two measurement intervals compared to previous measurements (1998–2004) because elevated mortality was observed with and without a wind event. Additionally, no major insect or disease outbreaks have been noted at the site. Therefore, *A. tsugense* was one of the likely components contributing to tree mortality.

A comparison of observed mortality rates (Figure 5) and predicted mortality rates based on tree growth (Figure 6) highlight the potential importance of other agents working in concert with *A. tsugense*. For observed tree mortality, heavily infected trees (DMR 6) exhibited the greatest mortality rates. After 2004, when mortality rates increased for all infection levels, mean annual mortality rates across plots were three to five times greater for heavily infected trees compared to uninfected trees (DMR 0). At a minimum, this indicates that heavy infection contributes to a substantial increase in tree mortality rates, if not being the ultimate cause. Figure 6 tells a similar story, but highlights that growth reductions due to *A. tsugense* appear to be associated with elevated mortality. In this case, differences between DMR 6 and DMR 0 were muted (50%–100% increase) both because the relative contribution of growth to the changes in mortality was only 23% and these differences in mortality were calculated for trees experiencing the mean growth rate for each DMR class, not the extreme low growth most associated with individual death. Differences between observed mortality (all mortality) and predicted mortality (mortality associated with DMR-related growth reductions) might represent interactions with additional agents, which are surely at work in these landscapes. Tree mortality is a consequence of complex biotic and abiotic factors and additional work is needed to not only assess the relative contribution of differing agents, but also their interactive role in tree death.

### ACKNOWLEDGEMENTS

We thank all the field personnel who collected data for this study. We also thank, the H. J. Andrews Long-Term Ecological Research (LTER) program (DEB-1440409), the University of Washington, and the USDA Forest Service Pacific Northwest Research Station for supporting this research. Data were provided by the Pacific Northwest Permanent Sample Plot Program at Oregon State University (<http://pnwpsp.forestry.oregonstate.edu/>). We thank Constance Harrington, James Guldin, Robert Shriver, and three anonymous reviewers for contributing reviews of this manuscript.

### ORCID

David M. Bell  <https://orcid.org/0000-0002-2673-5836>

## REFERENCES

- Agne, M. C., Beedlow, P. A., Shaw, D. C., Woodruff, D. R., Lee, E. H., Cline, S. P., & Comeleo, R. L. (2018). Interactions of predominant insects and diseases with climate change in Douglas-fir forests of western Oregon and Washington, U.S.A. *Forest Ecology and Management*, 409, 317–332. <https://doi.org/10.1016/j.foreco.2017.11.004>
- Allen, C. D., Breshears, D. D., & McDowell, N. G. (2015). On underestimation of global vulnerability to tree mortality and forest die-off from hotter drought in the Anthropocene. *Ecosphere*, 6(8), 129. <https://doi.org/10.1890/ES15-00203.1>
- Allen, C. D., Macalady, A. K., Chenchouni, H., Bachelet, D., McDowell, N., Vennetier, M., ... Cobb, N. (2010). A global overview of drought and heat-induced tree mortality reveals emerging climate change risks for forests. *Forest Ecology and Management*, 259, 660–684. <https://doi.org/10.1016/j.foreco.2009.09.001>
- Bell, D. M., Cohen, W. B., Reilly, M., & Yang, Z. (2018). Visual interpretation and time series modeling of Landsat imagery highlight drought's role in forest canopy declines. *Ecosphere*, 9(6), e02195. <https://doi.org/10.1002/ecs2.2195>
- Birch, J. D., Lutz, J. A., Hogg, E. H., Simard, S. W., Pelletier, R., LaRoi, G. H., & Karst, J. (2019). Decline of an ecotone forest: 50 years of demography in the southern boreal forest. *Ecosphere*, 10(4), e02698. <https://doi.org/10.1002/ecs2.2698>
- Chen, L., Huang, J., Dawson, A., Zhai, L., Stadt, K. J., Comeau, P. G., & Whitehouse, C. (2018). Contributions of insects and droughts to growth decline of trembling aspen mixed boreal forest of western Canada. *Global Change Biology*, 24(2), 655–667. <https://doi.org/10.1111/gcb.13855>
- Chmura, D. J., Anderson, P. D., Howe, G. T., Harrington, C. A., Halofsky, J. E., Peterson, D. L., ... Brad St.Clair, J. (2011). Forest responses to climate change in the northwestern United States: Ecophysiological foundations for adaptive management. *Forest Ecology and Management*, 261(7), 1121–1142. <https://doi.org/10.1016/j.foreco.2010.12.040>
- Choat, B., Jansen, S., Brodribb, T. J., Cochard, H., Delzon, S., Bhaskar, R., ... Zanne, A. E. (2012). Global convergence in the vulnerability of forests to drought. *Nature*, 491, 752–755. <https://doi.org/10.1038/nature11688>
- Clark, J. S., Iverson, L., Woodall, C. W., Allen, C. D., Bell, D. M., Bragg, D. C., ... Zimmermann, N. E. (2016). The impacts of increasing drought on forest dynamics, structure, and biodiversity in the United States. *Global Change Biology*, 22(7), 2329–2352. <https://doi.org/10.1111/gcb.13160>
- Cohen, W. B., Yang, Z., Stehman, S. V., Schroeder, T. A., Bell, D. M., Masek, J. G., ... Meigs, G. W. (2016). Forest disturbance across the conterminous United States from 1985–2012: The emerging dominance of forest decline. *Forest Ecology and Management*, 360, 242–252. <https://doi.org/10.1016/j.foreco.2015.10.042>
- Daly, C., Halbleib, M., Smith, J. I., Gibson, W. P., Doggett, M. K., Taylor, G. H., ... Pasteris, P. P. (2008). Physiographically sensitive mapping of climatological temperature and precipitation across the conterminous United States. *International Journal of Climatology*, 28(15), 2031–2064. <https://doi.org/10.1002/joc.1688>
- Das, A. J., & Stephenson, N. L. (2015). Improving estimates of tree mortality probability using potential growth rate. *Canadian Journal of Forest Research*, 45, 920–928. <https://doi.org/10.1139/cjfr-2014-0368>
- Das, A. J., Stephenson, N. L., & Davis, K. P. (2016). Why do trees die? Characterizing the drivers of background tree mortality. *Ecology*, 97(10), 2616–2627. <https://doi.org/10.1002/ecy.1497>
- Davis, R. J., Ohmann, J. L., Kennedy, R. E., Cohen, W. B., Gregory, M. J., Yang, Z., Spies, T. A. (2015). *Northwest Forest Plan—the first 20 years (1994–2013): Status and trends of late-successional and old-growth forests* (112 pp). General Technical Report PNW-GTR-911. Portland, OR: USDA Forest Service, Pacific Northwest Research Station. Retrieved from <http://www.treesearch.fs.fed.us/pubs/50060>
- Dobbertin, M., & Rigling, A. (2006). Pine mistletoe (*Viscum album* ssp. *austriacum*) contributes to Scots pine (*Pinus sylvestris*) mortality in the Rhone valley of Switzerland. *Forest Pathology*, 36(5), 309–322. <https://doi.org/10.1111/j.1439-0329.2006.00457.x>
- Fontúrbel, F. E., Lara, A., Lobos, D., & Little, C. (2018). The cascade impacts of climate change could threaten key ecological interactions. *Ecosphere*, 9(12), e02485. <https://doi.org/10.1002/ecs2.2485>
- Franklin, J. F., & DeBell, D. S. (1988). Thirty-six years of tree population change in an old-growth Pseudotsuga – Tsuga forest. *Canadian Journal of Forest Research*, 18, 633–639. <https://doi.org/10.1017/CBO9781107415324.004>
- Franklin, J. F., Shugart, H. H., & Harmon, M. E. (1987). Tree death as an ecological process. *BioScience*, 37(8), 550–556. <https://doi.org/10.2307/1310665>
- Geils, B. W., & Mathiasen, R. L. (1990). Intensification of dwarf mistletoe on southwestern Douglas-fir. *Forest Science*, 36(4), 955–969. <https://doi.org/10.1093/forestscience/36.4.955>
- Gray, A. N., & Whittier, T. R. (2014). Carbon stocks and changes on Pacific Northwest national forests and the role of disturbance, management, and growth. *Forest Ecology and Management*, 328, 167–178. <https://doi.org/10.1016/j.foreco.2014.05.015>
- Griebel, A., Watson, D., & Pendall, E. (2017). Mistletoe, friend and foe: Synthesizing ecosystem implications of mistletoe infection OPEN ACCESS Mistletoe, friend and foe: Synthesizing ecosystem implications of mistletoe infection. *Environmental Research Letters*, 12, 115012.
- Haavik, L. J., Billings, S. A., Guldin, J. M., & Stephen, F. M. (2015). Emergent insects, pathogens and drought shape changing patterns in oak decline in North America and Europe. *Forest Ecology and Management*, 354, 190–205. <https://doi.org/10.1016/j.foreco.2015.06.019>
- Hansen, E. M., Lewis, K. J., & Chastagner, G. A. (2018). *Compendium of conifer diseases*. St. Paul, MN: APS Press.
- Hawksworth, F. G. (1977). *The 6-class dwarf mistletoe rating system* (7 pp). General Technical Report RM-48. Fort Collins, CO: U.S. Department of Agriculture, Forest Service, Rocky Mountain Forest and Range Experiment Station.
- Hawksworth, F. G., & Wiens, D. (1996). *Dwarf mistletoes: Biology, pathology, and systematics* (410 pp). Agricultural Handbook 709. Washington, DC: USDA Forest Service. Retrieved from <https://www.fs.usda.gov/treesearch/pubs/4699>
- Hijmans, R. J., & van Etten, J. (2011). raster: Geographic analysis and modeling with raster data. *R Package Version 2.5-2*.
- Hillabrand, R. M., Lieffers, V. J., Hogg, E. H., Martínez-Sancho, E., Menzel, A., & Hacke, U. G. (2019). Functional xylem anatomy of aspen exhibits greater change due to insect defoliation than to drought. *Tree Physiology*, 39(1), 45–54. <https://doi.org/10.1093/treephys/tpy075>
- Hogg, E. H. (.), Brandt, J. P., & Michaelian, M. (2008). Impacts of a regional drought on the productivity, dieback, and biomass of western Canadian aspen forests. *Canadian Journal of Forest Research*, 38(6), 1373–1384. <https://doi.org/10.1139/X08-001>
- Kennedy, R. E., Ohmann, J., Gregory, M., Roberts, H., Yang, Z., Bell, D. M., ... Seidl, R. (2018). An empirical, integrated forest biomass monitoring system. *Environmental Research Letters*, 13, 041001. <https://doi.org/10.1088/1748-9326/aa9d9e>
- Kliejunas, J. T. (2009). *Review of literature on climate change and forest diseases of western North America* (54 pp). General Technical Report PSW-GTR-225. Albany, CA: USDA Forest Service, Pacific Southwest Research Station. <https://doi.org/10.2737/PSW-GTR-225>
- Kobe, R. K. (1996). Intraspecific variation in sapling mortality and growth predicts geographic variation in forest composition. *Ecological Monographs*, 66(2), 181–201. <https://doi.org/10.2307/2963474>
- Kolb, T. E., Fettig, C. J., Ayres, M. P., Bentz, B. J., Hicke, J. A., Mathiasen, R., ... Weed, A. S. (2016). Observed and anticipated impacts of

- drought on forest insects and diseases in the United States. *Forest Ecology and Management*, 380, 321–334. <https://doi.org/10.1016/J.FORECO.2016.04.051>
- Lloret, F., & Kitzberger, T. (2018). Historical and event-based bioclimatic suitability predicts regional forest vulnerability to compound effects of severe drought and bark beetle infestation. *Global Change Biology*, 24(5), 1952–1964. <https://doi.org/10.1111/gcb.14039>
- Marias, D. E., Meinzer, F. C., Woodruff, D. R., Shaw, D. C., Voelker, S. L., Brooks, J. R., ... McKay, J. (2014). Impacts of dwarf mistletoe on the physiology of host *Tsuga heterophylla* trees as recorded in tree-ring C and O stable isotopes. *Tree Physiology*, 34(6), 595–607. <https://doi.org/10.1093/treephys/tpu046>
- Mathiasen, R. L., Nickrent, D. L., Shaw, D. C., & Watson, D. M. (2008). Mistletoes: Pathology, systematics, ecology, and management. *Plant Disease*, 92(7), 988–1006. <https://doi.org/10.1094/PDIS-92-7-0988>
- Meinzer, F. C., Woodruff, D. R., & Shaw, D. C. (2004). Integrated responses of hydraulic architecture, water and carbon relations of western hemlock to dwarf mistletoe infection. *Plant, Cell and Environment*, 27, 937–946. <https://doi.org/10.1111/j.1365-3040.2004.01199.x>
- Mildrexler, D. J., Shaw, D. C., & Cohen, W. B. (2019). Short-term climate trends and the Swiss needle cast epidemic in Oregon's public and private coastal forestlands. *Forest Ecology and Management*, 432, 501–513. <https://doi.org/10.1016/J.FORECO.2018.09.025>
- Muir, J. A., & Hennon, P. E. (2007). *A synthesis of the literature on the biology, ecology, and management of western hemlock dwarf mistletoe* (142 pp). General Technical Report PNW-GTR-718. Portland, OR: USDA Forest Service, Pacific Northwest Research Station. <https://doi.org/10.2737/PNW-GTR-718>
- North, M., Chen, J., Oakley, B., Song, B., Rudnicki, M., Gray, A., & Innes, J. (2004). Forest stand structure and pattern of old-growth western hemlock/Douglas-fir and mixed-conifer forests. *Forest Science*, 50(3), 299–311. <https://doi.org/10.1093/forestscience/50.3.299>
- Plummer, M. (2014). *rjags: Bayesian graphical models using MCMC. R package version 3-13*. Retrieved from <https://cran.r-project.org/web/packages/rjags/index.html>
- Plummer, M. (2016). JAGS: Just another Gibbs sampler, version 4.1.0. Retrieved from <http://mcmc-jags.sourceforge.net/>
- PRISM Climate Group. (2018). 800-m PRISM gridded climate data. Oregon State University. Retrieved from <http://prism.oregonstate.edu>
- RDevelopmentCoreTeam. (2016). *R: A language and environment for statistical computing*. Version, 3.3.2. <https://doi.org/10.1007/978-3-540-74686-7>
- Reid, N., & Lange, R. T. (1988). Host specificity, dispersion and persistence through drought of two arid zone mistletoes. *Australian Journal of Botany*, 36, 299–313. <https://doi.org/10.1071/BT9880299>
- Robinson, D. C. E., & Geils, B. W. (2006). Modelling dwarf mistletoe at three scales: Life history, ballistics and contagion. *Ecological Modelling*, 199, 23–38. <https://doi.org/10.1016/j.ecolmodel.2006.06.007>
- Sangüesa-Barreda, G., Linares, J. C., & Camarero, J. J. (2012). Mistletoe effects on Scots pine decline following drought events: Insights from within-tree spatial patterns, growth and carbohydrates. *Tree Physiology*, 32(5), 585–598. <https://doi.org/10.1093/treephys/tps031>
- Sangüesa-Barreda, G., Linares, J. C., & Julio Camarero, J. (2013). Drought and mistletoe reduce growth and water-use efficiency of Scots pine. *Forest Ecology and Management*, 296, 64–73. <https://doi.org/10.1016/j.foreco.2013.01.028>
- Shaw, D. C., Chen, J., Freeman, E. A., & Braun, D. M. (2005). Spatial and population characteristics of dwarf mistletoe infected trees in an old-growth Douglas-fir – Western hemlock forest. *Canadian Journal of Forest Research*, 35(4), 990–1001. <https://doi.org/10.1139/x05-022>
- Shaw, D. C., & Franklin, J. F. (2019). *Long-term growth, mortality and regeneration of trees in permanent vegetation plots in the Pacific Northwest, 1910 to present*. Long-Term Ecological Research. Corvallis, OR: Forest Science Data Bank. [Database]. <https://doi.org/10.6073/pasta/2315afa15ad0a2317b49565da6258c47>
- Shaw, D. C., Franklin, J. F., Bible, K., Klopatek, J., Freeman, E., Greene, S., & Parker, G. G. (2004). Ecological setting of the Wind River old-growth forest. *Ecosystems*, 7(5), 427–439. <https://doi.org/10.1007/s10021-004-0135-6>
- Shaw, D., & Greene, S. (2003). Wind River Canopy Crane research facility and Wind River Experimental Forest. *The Bulletin of the Ecological Society of America*, 84(3), 115–121. [https://doi.org/10.1890/0012-9623\(2003\)84\[115:WRCCRF\]2.0.CO;2](https://doi.org/10.1890/0012-9623(2003)84[115:WRCCRF]2.0.CO;2)
- Shaw, D. C., Huso, M., & Bruner, H. (2008). Basal area growth impacts of dwarf mistletoe on western hemlock in an old-growth forest. *Canadian Journal of Forest Research*, 38(3), 576–583. <https://doi.org/10.1139/X07-174>
- Spiegelhalter, D. J., Best, N. G., Carlin, B. P., & Van Der Linde, A. (2002). Bayesian measures of model complexity and fit. *Journal of the Royal Statistical Society. Series B: Statistical Methodology*, 64, 583–639. <https://doi.org/10.1111/1467-9868.00353>
- Spurrer, S., & Smith, K. G. (2007). Desert mistletoe (*Phoradendron californicum*) infestation correlates with blue palo verde (*Cercidium floridum*) mortality during a severe drought in the Mojave desert. *Journal of Arid Environments*, 69(2), 189–197. <https://doi.org/10.1016/J.JARID ENV.2006.09.007>
- Stanton, S. (2007). Effects of dwarf mistletoe on climate response of mature ponderosa pine trees. *Tree-Ring Research*, 63(2), 69–80. <https://doi.org/10.3959/1536-1098-63.2.69>
- Swanson, M. E., Shaw, D. C., & Marosi, T. K. (2006). Distribution of western hemlock dwarf mistletoe (*Arceuthobium tsugense* [Rosendahl] G.N. Jones Subsp. *tsugense*) in mature and old-growth Douglas-fir (*Pseudotsuga menziesii* [Mirb.] Franco) forests. *Northwest Science*, 80(3), 207–217. Retrieved from <https://www.fs.usda.gov/treesearch/pubs/34606>
- Waring, R. H., & Franklin, J. F. (1979). Evergreen coniferous forests of the Pacific Northwest. *Science*, 204, 1380–1386. <https://doi.org/10.1126/science.204.4400.1380>
- Way, D. A. (2011). Parasitic plants and forests: A climate change perspective. *Tree Physiology*, 31(1), 1–2. <https://doi.org/10.1093/treephys/tpq113>

## SUPPORTING INFORMATION

Additional supporting information may be found online in the Supporting Information section at the end of the article.

**How to cite this article:** Bell DM, Pabst RJ, Shaw DC. Tree growth declines and mortality were associated with a parasitic plant during warm and dry climatic conditions in a temperate coniferous forest ecosystem. *Glob Change Biol*. 2019;00:1–11. <https://doi.org/10.1111/gcb.14834>